ANTIOXIDANTS & REDOX SIGNALING
Volume 30, Number 13, 2019

DOI: 10.1089/ars.2018.7542

Discoveries

ORIGINAL RESEARCH COMMUNICATION

Adaptor Protein p66Shc: A Link Between Cytosolic and Mitochondrial Dysfunction in the Development of Diabetic Retinopathy

Manish Mishra,[1] Arul J. Duraisamy,[1] Sudarshan Bhattacharjee,[1] and Renu A. Kowluru[1,2]

Abstract

Aims: Diabetes increases oxidative stress in the retina and dysfunctions their mitochondria, accelerating capillary cell apoptosis. A 66 kDa adaptor protein, p66Shc, is considered as a sensor of oxidative stress-induced apoptosis. In the pathogenesis of diabetic retinopathy, a progressive disease, reactive oxygen species (ROS) production by activation of a small molecular weight G-protein (Ras-related C3 botulinum toxin substrate 1 [Rac1])-Nox2 signaling precedes mitochondrial damage. Rac1 activation is facilitated by guanine exchange factors (GEFs), and p66Shc increases Rac1-specific GEF activity of Son of Sevenless 1 (Sos1). p66Shc also possesses oxidoreductase activity and can directly stimulate mitochondrial ROS generation. Our aim was to investigate the role of p66Shc in the development of diabetic retinopathy and mechanism of its transcription.

Results: High glucose increased p66Shc expression in human retinal endothelial cells, and elevated acetylated histone 3 lysine 9 (H3K9) levels and transcriptional factor p53 binding at its promoter. Glucose also augmented interactions between Rac1 and Sos1 and activated Rac1-Nox2. Phosphorylation of p66Shc was increased, allowing it to interact with peptidyl prolyl isomerase to facilitate its localization inside the mitochondria, culminating in mitochondrial damage. *P66shc*-small interfering RNA (siRNA) inhibited glucose-induced Rac1 activation and mitochondrial damage. Similar results are observed in retinal microvessels from diabetic rats.

Innovation: This is the first report identifying the role of p66Shc in the development of diabetic retinopathy and implicating increased histone acetylation in its transcriptional regulation.

Conclusion: Thus, p66Shc has dual role in the development of diabetic retinopathy; its regulation in the early stages of the disease should impede Rac1-ROS production and, in the later stages, prevent mitochondrial damage and initiation of a futile cycle of free radicals. *Antioxid. Redox Signal.* 30, 1621–1634.

Keywords: adaptor protein p66Shc, diabetic retinopathy, mitochondria, reactive oxygen species, Ras-related C3 botulinum toxin substrate, Rac1

Introduction

DIABETIC RETINOPATHY, ONE OF THE serious microvascular complications, is the leading cause of acquired blindness in working aging adults. Hyperglycemia induces metabolic abnormalities and alters many genes associated with these abnormalities (16, 18). Oxidative stress is increased in the retina and its capillary cells, and the mitochondria become dysfunctional, accelerating apoptosis of capillary cells, a phenomenon that precedes the development of vascular histopathology characteristic of diabetic retinopathy (18, 43). Reactive oxygen species (ROS) are important mediators of vascular dysfunction, and a 66 kDa proto-oncogene Src homologous-collagen (Shc) homologue adaptor protein, p66Shc, is considered as a sensor of oxidative stress-induced apoptosis (17, 47). In diabetic patients, the expression of p66Shc in mononuclear cells is shown to correlate with the plasma 8-isoprostane, a marker of oxidative stress (45), and in patients with nephropathy, with the levels of low-density lipoproteins, blood glucose levels, and duration of diabetes (61). Downregulation of p66Shc in mesangial cells is associated with reduced susceptibility to oxidative stress and amelioration of diabetic glomerulopathy (38), and decrease in

Departments of [1]Ophthalmology and [2]Anatomy/Cell Biology, Kresge Eye Institute, Wayne State University, Detroit, Michigan.

Innovation

Early activation of cytosolic Ras-related C3 botulinum toxin substrate 1 (Rac1)-NADPH oxidase (Nox)2-reactive oxygen species (ROS) signaling axis leads to mitochondrial damage, activating a self-perpetuating cycle of mitochondrial ROS, which plays a critical role in development of diabetic retinopathy. How cytosolic disturbances lead to the mitochondrial dysfunction, however, remains obscure. This is the first report documenting p66Shc as a link between cytosolic and mitochondrial dysfunction in the development of diabetic retinopathy. We show that due to Sirtuin 1 (Sirt1) inhibition in hyperglycemia, *p66Shc* promoter is hyperacetylated, which increases transcriptional factor p53 binding. Activated p66Shc, *via* activating Rac1-Nox2 signaling, elevates cytosolic ROS, and by increasing interactions between phosphorylated p66Shc and peptidyl-prolyl cis/trans isomerase 1 (Pin1), increases mitochondrial ROS.

p66Shc by Sirtuin 1 (Sirt1) is shown to prevent hyperglycemia-induced endothelial dysfunction (62). However, the role of p66Shc in the development of diabetic retinopathy remains unclear.

Although mitochondria are the major source of ROS, free radicals are also generated by cytosolic NADPH oxidases (Noxs), and diabetic environment activates phagocyte-like Nox2 and Nox4 in the retina and its capillary cells (32, 36). Nox2 is a multiprotein membrane-bound complex, and Ras-related C3 botulinum toxin substrate 1 (Rac1) is essential for its activation (50). Activated Rac1 moves to the cell membrane, where it binds with the Nox2 complex to generate ROS; in diabetic retinopathy, Rac1-Nox2-mediated ROS generation leads to the mitochondrial damage (32, 33). The activity of Rac1 is governed by several guanine exchange factors (GEFs) including Tiam1 and Son of Sevenless 1 (Sos1). P66Shc also induces Rac1 activation, and this is mediated *via* its effect on Rac1-specific Sos1 (4, 21). P66Shc-mediated activation of Rac1 is facilitated by decreased binding of Sos1 with the growth factor receptor-bound protein 2 (Grb2) (24, 27). However, the role of p66Shc in the regulation of Sos1-Rac1-Nox2-ROS signaling in diabetic retinopathy remains to be investigated.

The function of p66Shc is regulated at both transcriptional and post-translational levels (35, 57); although histone acetylation activates gene expression, deacetylation suppresses the expression (51). Diabetes-induced expression of *p66Shc* in human umbilical vein endothelial cells is considered to be mediated by acetylation of histone 3-in its promoter (62). Furthermore, Sirt1, a class III histone deacetylase, is inactivated in the retina in diabetes, and its overexpression prevents mitochondrial damage and the development of retinopathy in diabetic mice (39). P66Shc is also a downstream target of the tumor suppressor transcription factor p53, defects in p53-p66Shc apoptotic pathway are considered to play a major role in p66Shc-mediated tumor initiation, and acetylation of p53 is critical in its regulation of *p66Shc* expression (3, 7, 57). How diabetes regulates p66Shc in the retina is not clear.

P66Shc has an oxidoreductase activity, and it can directly stimulate mitochondrial ROS generation; localization of p66Shc in the mitochondrial membrane oxidizes cytochrome c (Cyt c), generating ROS (19). Translocation of p66Shc into the mitochondria is facilitated by phosphorylation of its Serine 36 by protein kinase C, β isoform (PKCβ) (48), and diabetes activates PKCβ in the retina and its capillary cells (30). Phosphorylated p66Shc increases its affinity toward peptidyl prolyl isomerase, peptidyl-prolyl cis/trans isomerase 1 (Pin1), which isomerizes p66Shc, and isomerization is essential for its translocation into the mitochondria (15, 48); blood monocytes from diabetic patients have increased Pin1 (46). Whether p66Shc has any role in mitochondrial damage, associated with the development of diabetic retinopathy, is elusive.

This study aims to understand the mechanism responsible for p66Shc regulation and examine its role in regulating cytosolic and mitochondrial ROS in the development of diabetic retinopathy. Using human retinal endothelial cells (HRECs), we have investigated the effect of hyperglycemia on p66Shc-Rac1-ROS signaling and mitochondrial damage. The specific role of p66Shc in activation of cytosolic and mitochondrial ROS was confirmed using genetically modified HRECs. Key parameters of p66Shc-Rac1-ROS signaling were validated in the retinal microvessels, the site of histopathology associated with diabetic retinopathy (16), from streptozotocin-induced diabetic rats.

Results

Compared with that of cells in normal glucose, incubation of endothelial cells in high glucose for 96 h increased *p66Shc* gene transcripts by $\sim$2.5-fold, and this was accompanied by a $\sim$75% increase in its protein expression (Fig. 1a, b and Supplementary Fig. S1). However, incubation of cells in 20 m*M* L-glucose had no effect on p66Shc expression.

Since p66Shc is an important regulator of Rac1 (23), and activation of Rac1 is an early event in the development of diabetic retinopathy (32), temporal relationship between exposures of cells to high glucose and *p66Shc* was investigated. As shown in Figure 1c, compared with the cells in normal glucose, increase in *p66Shc* transcripts was observed within 24 h of glucose insult. Consistent with increase in *p66Shc*, as expected (32, 33), significant increases in Rac1 activity and ROS were also observed in the same samples, and they all remain elevated at least till 96 h of high glucose insult. The correlation analysis of the temporal relationship of *p66Shc* with Rac1-ROS showed a strong correlation coefficient among these three parameters (>0.96).

The role of p66Shc in the regulation on Rac1 activation was determined in the cells transfected with *p66Shc*-small interfering RNA (siRNA); Figure 1d shows >40% decrease in *p66Shc* transcripts in *p66Shc*-siRNA transfected cells. Consistent with the inhibition of glucose-induced increase in oxidative stress by Rac1-Nox inhibitor (32) and by overexpression of *Sod2* (a gene encoding for mitochondrial superoxide dismutase) (29), *p66Shc*-siRNA also attenuated glucose-induced increase of Rac1 and ROS (Fig. 1e, f). Furthermore, *p66Shc*-siRNA also significantly ameliorated increase in oxidatively modified DNA, as shown by decreased levels of 8-OHdG in *p66Shc*-siRNA transfected cells, compared with untransfected cells, exposed to high glucose (Fig. 1g). However, the cells transfected with scrambled siRNA control incubated in high glucose, or *p66Shc*-siRNA

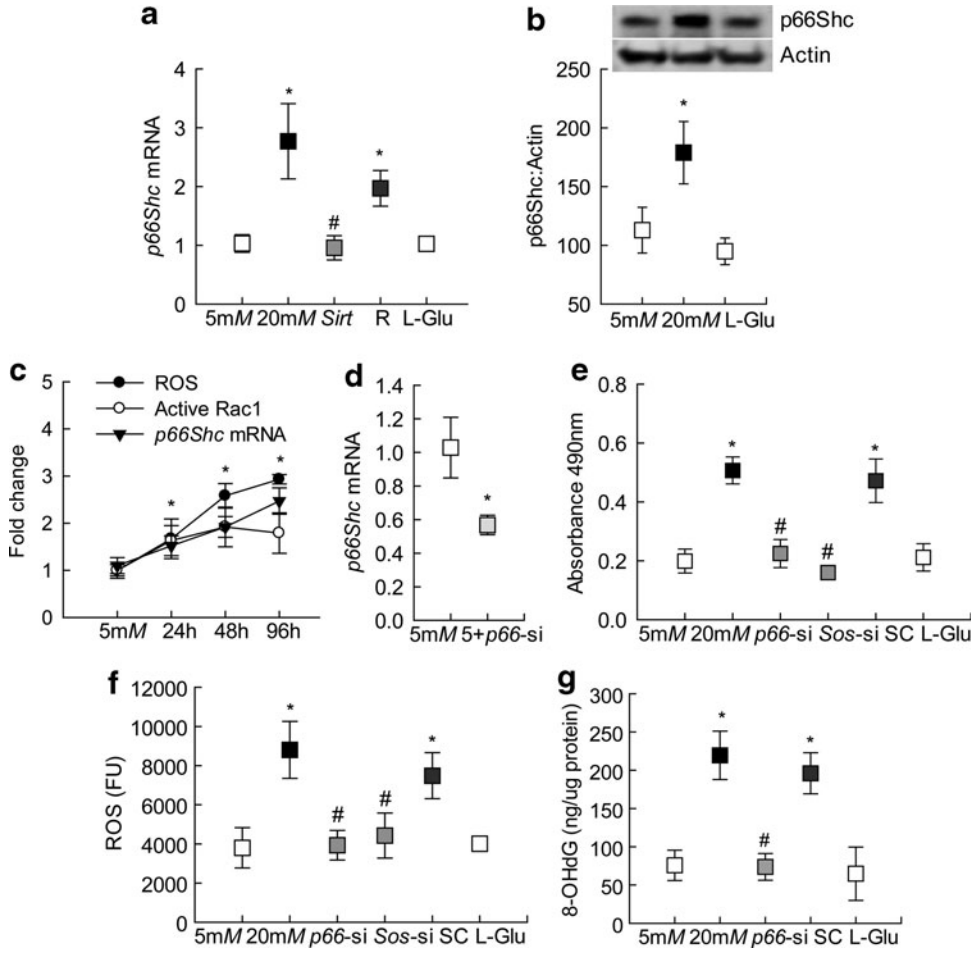

FIG. 1. Effect of *p66Shc* on the glucose-induced Rac1 activation and ROS levels. HRECs exposed to high or normal glucose for 96 h were analyzed for p66Shc **(a)** mRNA and **(b)** protein levels using qPCR and Western blot techniques, respectively. β-Actin was used as an internal control. Supplementary Figure S1 showing uncropped p66Shc and actin Western blots from three different preparations. **(c)** Cells incubated with 20 m*M* glucose for 24–96 h were used to investigate the temporal relationship with *p66Shc* gene transcripts, active Rac1 and ROS, and potential correlation was determined by analyzing correlation coefficient. **(d)** Transfection efficiency of *p66*-siRNA was quantified by qPCR. **(e)** Active Rac1 was quantified in 20 μg protein by a G-LISA colorimetric assay and absorbance at 490 nm was plotted. **(f)** Total ROS levels were quantified fluorometrically in 5 μg protein using DCFH-DA fluorescence dye, and the graph shows absolute fluorescence intensity obtained in each sample. **(g)** 8-OHdG levels were measured in the total genomic DNA by an ELISA method. Each measurement was made in duplicate in four to five samples per group. The values obtained from cells in 5 m*M* glucose are considered as 1 (or 100%) and are represented as mean ± SD. Five millimolars and 20m*M* represent cells in 5 or 20 m*M* glucose; *Sirt* and R represent cells transfected with *Sirt1* cDNA or with transfection reagent alone, and incubated in 20 m*M* glucose; *p66*-si, *Sos*-si, or SC represents cells transfected with *p66Shc* siRNA, *Sos1* siRNA, or scrambled RNA respectively, and incubated in 20 m*M* glucose; 5+*p66*-si represents cells transfected with *p66Shc* siRNA and incubated in 5 m*M* glucose; L-Glu represents 20 m*M* L-glucose. $^{*}p < 0.05$ *versus* 5 m*M* glucose and $^{\#}p < 0.05$ *versus* 20 m*M* glucose. cDNA, complementary DNA; DCFH-DA, dichlorodihydrofluorescein diacetate; ELISA, enzyme-linked immunosorbent assay; HRECs, human retinal endothelial cells; mRNA, messenger RNA; qPCR, quantitative real-time polymerase chain reaction; Rac1, Ras-related C3 botulinum toxin substrate 1; ROS, reactive oxygen species; SC, scrambled RNA; SD, standard deviation; siRNA, small interfering RNA.

transfected cells incubated in normal glucose medium, had no change in their phenotype, and the values were similar to those obtained from the untransfected cells incubated in high glucose or in normal glucose, respectively.

Regulation of p66Shc *transcription*

Since *p66Shc* is a target of transcription factor p53 (57), p53 binding at *p66Shc* promoter was investigated. Compared with that of cells in normal glucose, p53 binding was increased by approximately twofold in the cells incubated in high glucose; the IgG controls in the same samples were <0.5% of those obtained from p53 antibody (Fig. 2a). Since acetylation of p53 is important in regulating its transcriptional activity, and diabetes inhibits deacetylase Sirt1 in the retina (39, 56), the effect of overexpression of *Sirt1* on p53 binding at *p66Shc* promoter was determined. *Sirt1* overexpression prevented glucose-induced increase in p53 binding (Fig. 2a). In the same cell preparations, *Sirt1* overexpression also prevented increase in *p66Shc* transcription (Fig. 1a). The values

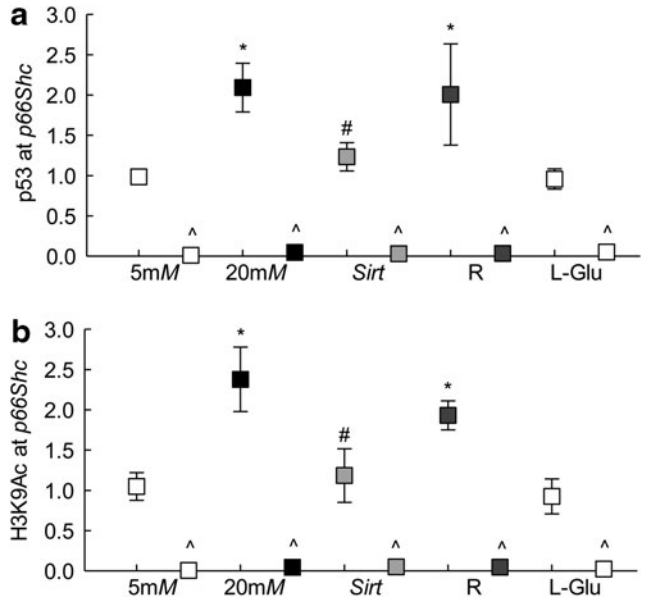

FIG. 2. Binding of p53 and acetylated H3K9 at p66Shc promoter. HRECs, incubated in high glucose for 96 h, were analyzed for **(a)** p53 binding and **(b)** H3K9Ac by ChIP technique using IgG as an antibody control (indicated as ^). Each measurement was made in duplicate in three to four samples per group, and values obtained from cells in 5 m*M* glucose are considered as 1.5 and 20 m*M* representing 5 or 20 m*M* glucose; L-Glu represents 20 m*M* L-glucose; *Sirt* and R represent cells transfected with *Sirt1* cDNA or with transfection reagent alone, and incubated in 20 m*M* glucose for 96 h. * and $^{\#}p < 0.05$ compared with cells in 5 or 20 m*M* glucose, respectively. ChIP, chromatin immunoprecipitation; H3K9Ac, histone 3 lysine 9 acetylation; Sirt1, sirtuin 1.

obtained from the cells incubated with transfection reagent alone or untransfected cells, incubated in high glucose, were not different from each other.

Post-translational modifications of histones play an important role in regulating binding of the transcription factors, and acetylation of histones at the gene promoter is related to activate gene transcription (6, 22, 49). To investigate the role of histone acetylation in *p66Shc* transcription, histone 3 lysine 9 acetylation (H3K9Ac) levels were quantified at its promoter. Incubation of cells in high glucose for 96 h, compared with that of cells in normal glucose, elevated H3K9Ac levels at *p66Shc* promoter by ~2.5-fold, and this increase was ameliorated by overexpression of *Sirt1*. Cells incubated in 20 m*M* L-glucose had no effect on H3K9Ac levels (Fig. 2b).

p66Shc-Rac1 regulation

P66Shc increases active Rac1 by augmenting Rac1-specific activity of Sos1 (23); to determine the role of Sos1 in p66Shc-mediated Rac1 activation, the binding of Rac1 with Sos1 was investigated. Coimmunoprecipitation experiments showed increased binding of Rac1-Sos1 in cells exposed to high glucose for 96 h, and glucose-induced increased Rac1-Sos1 interactions were attenuated by *p66Shc*-siRNA (Fig. 3a and Supplementary Fig. S2). Consistent with this, immunofluorescence technique also showed increased colocalization of Rac1-Sos1 (Fig. 3b). This increased Rac1-Sos1 association was observed despite any significant increase in glucose-induced *Sos1* transcription. Interestingly, *Sos1*-siRNA ameliorated glucose-induced increase in active Rac1 and ROS levels (Fig. 1e, f). As a measure of transfection efficiency, *Sos1*-siRNA transfected cells had ~50% decrease in *Sos1* transcript levels (Fig. 3c).

Since p66Shc activates Rac1 by decreasing Sos1 binding with Grb2 (23), effect of high glucose on Sos1-Grb2 binding was investigated. Compared with cells in normal glucose or in 20 m*M* L-glucose, coimmunoprecipitation results showed 40% decrease in Sos1-Grb2 interactions in cells incubated in high glucose, and this decrease in Sos1-Grb2 binding was prevented by *p66Shc*-siRNA, but not by scrambled RNA. Consistent with Sos1 expression, high glucose also had no effect on Grb1 messenger RNA (mRNA) or protein expression (Fig. 4a, b and Supplementary Figs. S3 and S4).

p66Shc and mitochondrial ROS

To investigate the role of p66Shc in glucose-induced increased mitochondrial damage, its translocation inside the mitochondria was determined. As shown in Figure 5a, localization of p66Shc inside the mitochondria was more than twofold higher in the cells incubated in high glucose for 96 h compared with cells incubated in normal glucose or 20 m*M* L-glucose. Both immunohistochemical technique and enzyme-linked immunosorbent assay (ELISA) showed attenuation of glucose-induced mitochondrial ROS by *p66Shc*-siRNA (Fig. 5b, c). Consistent with ROS, *p66Shc*-siRNA also prevented increase in mitochondrial DNA (mtDNA) damage and capillary cell apoptosis; the values obtained from *p66Shc*-siRNA transfected cells were not different from those observed from untransfected cells in normal glucose (Fig. 5d, e).

Phosphorylation of p66Shc is associated with its mitochondrial localization (19); phosphorylated p66Shc binds with Pin1 for isomerization, which is critical for its mitochondrial translocation. However, phosphorylated p66Shc is first dephosphorylated before it can be translocated inside the mitochondria (17, 48). Quantification of p66Shc phosphorylation by both Western blotting and immunostaining showed significant increase in phosphorylated p66Shc in the cells exposed to high glucose compared with the cells exposed to normal glucose or 20 m*M* L-glucose (Fig. 6a, b and Supplementary Fig. S5). Consistent with increase in phosphorylated p66Shc, high glucose also increased the gene transcripts of *Pin1* by approximately twofold (Fig. 6c).

To confirm the role of Pin1 in mitochondrial ROS, cells transfected with *Pin1*-siRNA were analyzed for mitochondrial ROS levels, and as shown in Figure 5b–d, *Pin1*-siRNA transfected cells showed significant reduction in mitochondrial ROS levels and mtDNA damage compared with untransfected cells in high glucose for 96 h.

Rat retinal microvessels

Consistent with the results from endothelial cells, diabetes increased gene transcripts of *p66Shc* in rat retinal microvessels (Fig. 7a). Compared with the age-matched normal rats, although Sos1 expression was not significantly increased in diabetic rats, immunofluorescence microscopy showed a significant increase in the cellular localization of Sos1 with Rac1 (Fig. 7a, b). This diabetes-induced increase in p66Shc was accompanied by a significant increase in p53 binding and H3K9Ac levels at its promoter (Fig. 7c, d).

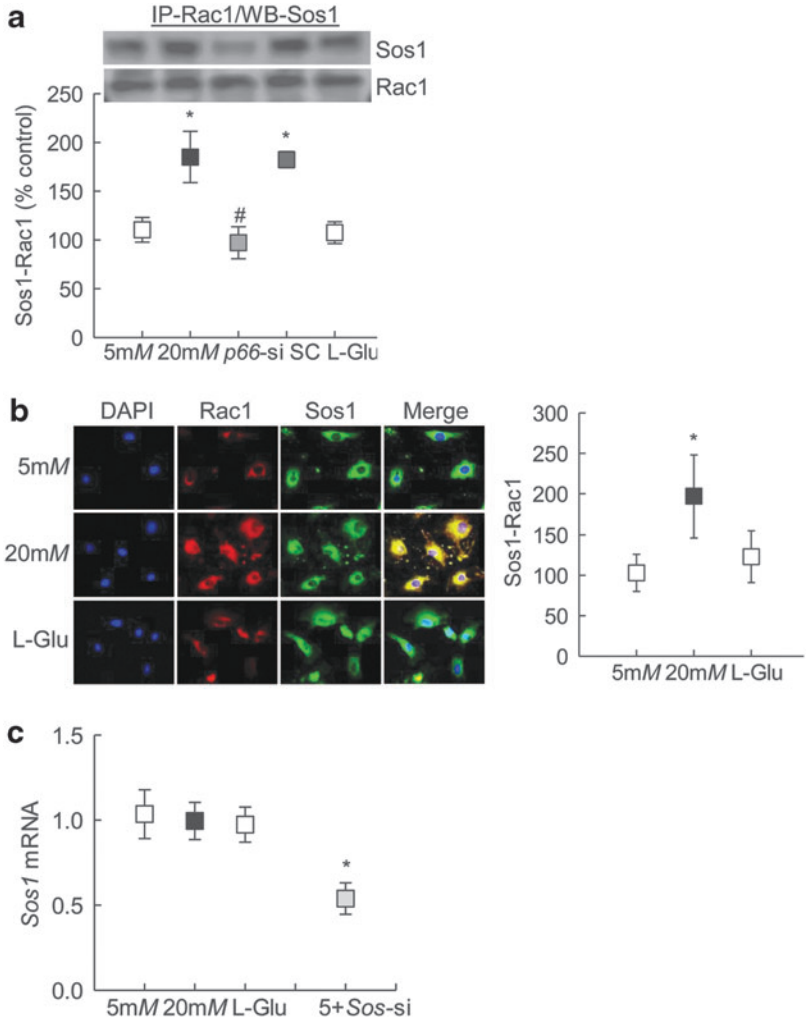

FIG. 3. Effect of *p66Shc* regulation on glucose-induced Rac1 activation and its binding with Sos1. Cells transfected with *p66*-siRNA, and incubated in 20 m*M* glucose for 96 h, were for analyzed for **(a)** Rac1 binding with Sos1 by immunoprecipitating Rac1, followed by Western blotting for Sos1 (Supplementary Fig. S2). Supplementary Figure S2 for uncropped Sos1 and Rac1 Western blots from three different samples. **(b)** Cellular colocalization of Rac1 with Sos1 was determined by immunofluorescence using Texas Red (*red*) and Alexa-Flour 488 (*green*) conjugated secondary antibody, respectively. Fluorescence intensity for colocalized Rac1 and Sos1 was quantified using AxioVision Rel. 4.8 imaging analysis software. **(c)** Sos1 transcripts were quantified by qPCR using β-Actin as an internal control. The values obtained from cells in 5 m*M* glucose are considered as 1 (or 100%), and are represented as mean ± SD from —three to five samples per group. Five millimolars and 20 m*M* represent 5 or 20 m*M* glucose; L-Glu represents 20 m*M* L-glucose; *p66*-si or SC represents cells transfected with *p66Shc* siRNA or scrambled RNA, respectively, and incubated in 20 m*M* glucose for 96 h; 5+*Sos*-si represents cells transfected with *Sos1* siRNA and incubated in 5 m*M* glucose. $^{*}p < 0.05$ *versus* 5 m*M* glucose and $^{\#}p < 0.05$ *versus* 20 m*M* glucose. Sos1, Son of Sevenless 1.

Retinal cryosections from diabetic rats, compared with those from normal rats, had increased mitochondrial localization of p66Shc (Fig. 8a), and increased colocalization of Pin1 with phosphorylated p66Shc (Fig. 8b). Similarly, *Pin1* transcripts were also increased significantly in the retinal microvessels from the same diabetic rats (Fig. 8c).

Discussion

Excessive intracellular ROS generation is considered as a common pathway in hyperglycemia-induced retinal injury, and oxidative stress in diabetic patients is relatively high than in healthy individuals (18, 45). P66Shc is known to regulate both cellular and mitochondrial ROS levels by regulating Rac1 activation and by affecting the mitochondrial electron transport chain system, respectively (17). We have shown that in diabetes, active Rac1 is elevated in the retina, which activates Nox2-mediated cytosolic ROS production, and subsequently damages the mitochondria, leading to capillary cell apoptosis (32, 33). In this study, using models of diabetic models of diabetic retinopathy, our results show that in the hyperglycemic condition, p66Shc, its binding with Grb2 and with Sos1, and active Rac1 are increased. Owing to decreased Sirt1, H3K9 remains acetylated, facilitating p53 binding at *p66Shc* promoter and activating its transcription, and overexpression of *Sirt1* ameliorates this. We also show that p66Shc is phosphorylated, which increases its binding with Pin1 and elevates p66Shc levels inside the mitochondria,

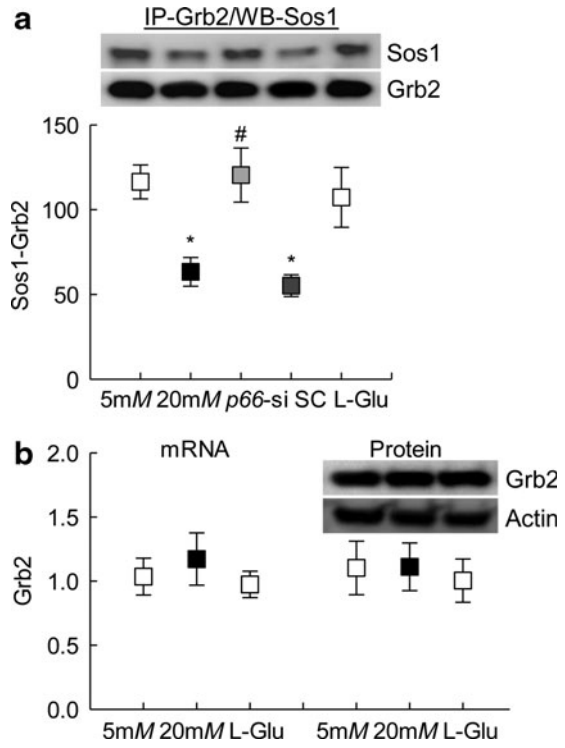

FIG. 4. Regulation of *p66Shc* and its effect on glucose-induced Grb2-Sos1 binding. (a) HRECs transfected with *p66*-siRNA, and incubated in 20 m*M* glucose, were analyzed for the Grb2 binding with Sos1 by immunoprecipitating Grb2, and Western blotting for Sos1. Supplementary Figure S3 shows the uncropped Sos1 and Grb2 Western blots from three samples. **(b)** Expression of Grb2 was quantified at mRNA and protein levels using qPCR and Western blot techniques, respectively. β-Actin was used as an internal control. Supplementary Figure S4 depicts uncropped Grb2 and actin Western blots from three different preparations. Each measurement was made in duplicate, and the values are mean ± SD from four to five samples per group. The values obtained from cells in 5 m*M* glucose are considered as 1 (or 100%). Five millimolars and 20 m*M* represent 5 or 20 m*M* glucose; L-Glu represents 20 m*M* L-glucose; *p66*-si or SC represents cells transfected with *p66Shc* siRNA or scrambled RNA, respectively, and incubated in 20 m*M* glucose for 96 h. * and $^{\#}p < 0.05$ compared with cells in 5 or 20 m*M* glucose, respectively. Grb2, growth factor receptor-bound protein 2.

resulting in increased mitochondrial ROS levels. These results clearly suggest that p66Shc is a critical player in the development of diabetic retinopathy.

ROS are considered as one of the major regulators of cellular processes (12, 32), and cytosolic ROS generation, *via* activation of Nox, plays a crucial role in mitochondrial ROS generation, initiating a vicious cycle of ROS-induced ROS (11–13, 26, 37, 53, 63, 64). Generation of cytosolic and mitochondrial ROS has significant interactions in many diseases including in diabetic retinopathy (32). In this study, we highlight the role of p66Shc in cytosolic-mitochondrial ROS production. P66Shc is one of the three isoforms of the ShcA adaptor protein family, and although the other two members, p46Shc and p52Shc, are ubiquitously expressed, p66Shc has constrained expression (1, 5). Both p46Shc and p52Shc isoforms function as cytoplasmic signal transducers and link activated receptor tyrosine kinases to the Ras pathway by recruitment of the Grb2–Sos1 complex. However, p66Shc has an extra N-terminal collagen homology-2 domain (CH2 domain), and by displacing Sos1 from its complex with Grb2, it inhibits Ras activation and increases cytosolic oxidative stress by activating Rac1-specific GEF activity of Sos1 (2, 23). Rac1 activation in the retina and its vasculature in diabetes are intimately associated with increased cytosolic ROS, and inhibition of Rac1-Nox2 axis in mice by NSC23766, an inhibitor of Rac1-GEF, Tiam1, in addition to inhibiting Rac1 activation, also inhibits Nox2-ROS generation (32, 33). In this study, we show that p66Shc expression is increased by hyperglycemia. Although hyperglycemia did not alter Sos1 and Grb2 expression, inhibition of p66Shc by its specific siRNA prevented glucose-induced increased binding of Sos1 with Rac1, and ameliorated decrease in Sos1 binding with Grb2, suggesting a significant role of Grb2-Sos1 in regulation of p66Shc-mediated Rac1-ROS signaling. Rac1 can also increase the stability of p66Shc by forming a feedback loop to maintain cellular ROS production (24); the role of Rac1 in maintaining p66Shc stability, however, cannot be ruled out.

P66Shc is tightly regulated at the transcriptional (57) and post-translational levels (35), and it has multiple transcription factor binding sites (42, 57). *P66Shc* promoter has a p53 response element, and p53, an important transcription factor, is shown to regulate *p66Shc* expression, including in many disease conditions such as cancer and diabetes (5, 8, 25, 59). In this study, we show that the binding of p53 at *p66Shc* promoter is increased in hyperglycemic medium. Binding of transcription factor is regulated by epigenetic modifications (6, 49), our results show that the levels of H3K9Ac are significantly elevated at *p66Shc* promoter. In support of this, increase in histone 3 acetylation is associated with the low-density lipoprotein-induced upregulation of *p66Shc* in human vascular cells (60, 62). Others have also shown a crosstalk between histone methylation and histone acetylation at the *p66Shc* promoter in visceral fat arteries, but, contrary to our results, H3K9Ac is decreased in obese mice (10). Since histone deacetylases are tissue specific (58), the possibility that histone deacetylating machinery is differentially regulated in visceral fat and retinal vasculature cannot be ruled out. Sirt1 activity is significantly decreased in the retinal vasculature in diabetes, and its overexpression in mice ameliorates retinal vascular and neuronal abnormalities associated with diabetic retinopathy (39). The results presented here clearly show that *Sirt1* overexpression, *via* regulating acetylation of histones at *p66Shc* promoter, prevents p53 binding and regulates its transcription. We recognize that p66Shc is also a direct target of Sirt1, and Sirt1-mediated p66Shc post-translational acetylation at lysine 81 can regulate oxidative stress and endothelial dysfunction in diabetes (35), the role of Sirt1 in direct regulation p66Shc needs further investigation.

Although p66Shc increases cytosolic oxidative stress, ROS, in turn, also promote mitochondrial translocation of p66Shc, and once inside the mitochondria, p66Shc interacts with Cyt c (a membrane-bound electron carrier), serving as a redox enzyme to transfer electrons from reduced Cyt c to oxygen (19). Incomplete oxygen reduction leads to ROS production, which, in turn, promotes the formation of a permeability-transition pore in mitochondrial membrane, releasing Cyt c into the cytoplasm and, subsequently, activating the apoptotic machinery (55). In the development of diabetic retinopathy, mitochondrial

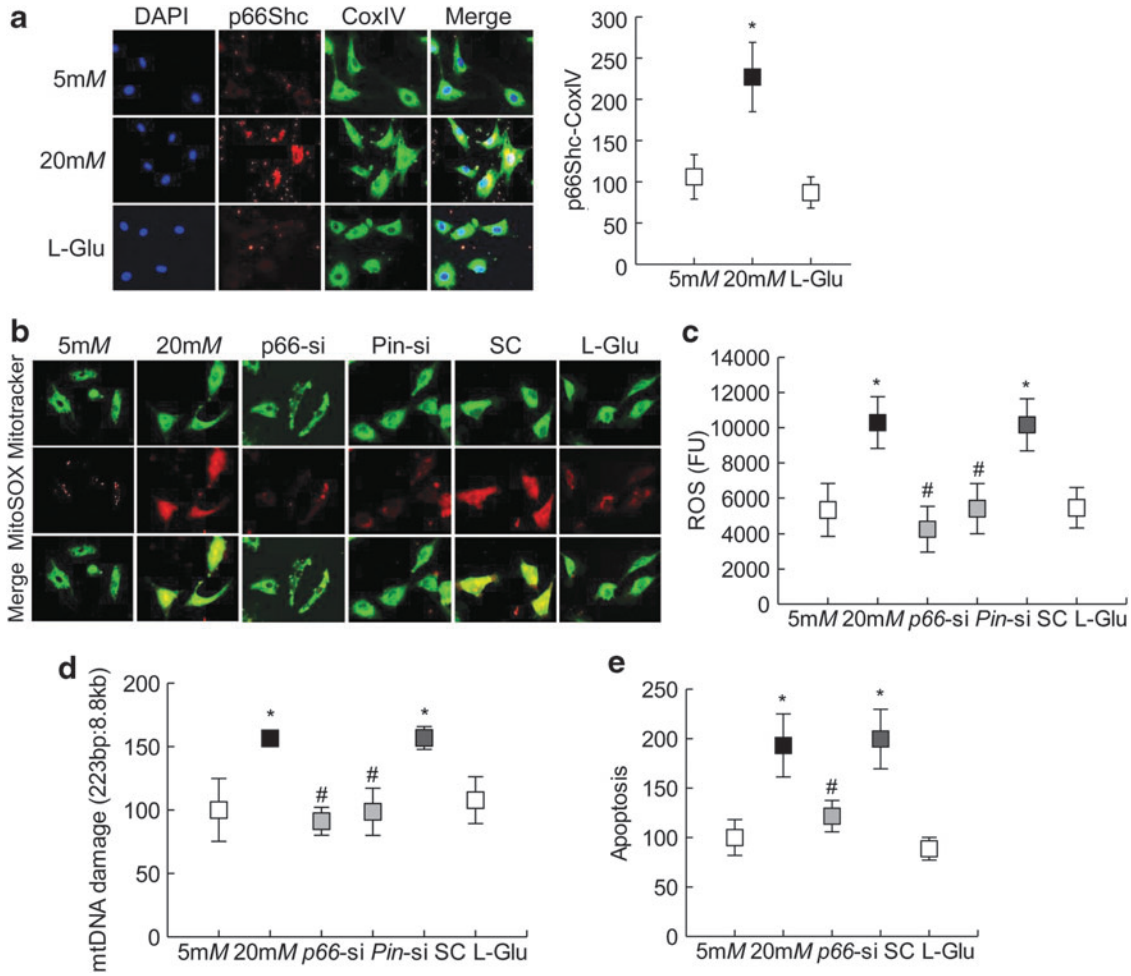

FIG. 5. Mitochondrial localization of *p66Shc*. **(a)** Mitochondrial localization of p66Shc was determined in HRECs exposed to high glucose for 96 h by immunofluorescence using Texas Red (*red*) and DyLight 488 (*green*) conjugated secondary antibodies for p66Shc, and CoxIV was used as a mitochondrial marker, respectively. Fluorescence intensity for colocalized p66Shc-CoxIV was quantified. Mitochondrial ROS were quantified by **(b)** immunofluorescence imaging using mitochondrial permeable MitoSOX™ (*red*) dye and mitotracker (*green*), and **(c)** fluorometrically on a plate reader using 5 μg of mitochondrial protein and 4 μM DCFH-DA dye, the graph shows absolute fluorescence intensity obtained in each sample. **(d)** Mitochondrial DNA damage was assessed by extended-length PCR using semiquantitative PCR. **(e)** Apoptosis was quantified by an ELISA kit for histone-associated DNA fragments. Each measurement was made in duplicate in four to five samples per group, and the values obtained from cells in 5 mM glucose are considered as 100. Five millimolars and 20 mM represent 5 or 20 mM glucose; L-Glu represents 20 mM L-glucose; *p66*-si, *Pin*-si or SC represents cells transfected with *p66Shc* siRNA, *Pin1* siRNA, or scrambled RNA, respectively, and incubated in 20 mM glucose for 96 h. $^{*}p < 0.05$ *versus* 5 mM glucose and $^{\#}p < 0.05$ *versus* 20 mM glucose.

damage plays a critical role; retinal mitochondria are dysfunctional before appearance of apoptotic cells and capillary degeneration (28, 32). mtDNA copy numbers are decreased, and damaged mtDNA, *via* compromising the electron transport chain system, continues to fuel into the vicious cycle of free radicals (40). Results presented here show that the inhibition of p66Shc also significantly reduces mitochondrial damage.

The CH2 domain of p66Shc contains a crucial serine 36 residue, which is phosphorylated in response to oxidative stress (17). Phosphorylation of p66Shc is mediated by the activation of PKCβ (48), and conformational changes in p66Shc increase its affinity toward Pin1, isomerizing p66Shc and facilitating its mitochondrial transportation (48). PKCβ is activated in the retinal vasculature in diabetes, and is implicated with retinal hemodynamic and molecular abnormalities associated with the development of diabetic retinopathy (30). In this study, our results showing increased mitochondrial localization of p66Shc and serine 36 phosphorylation clearly suggest the role of p66Shc in regulation of mitochondrial ROS and mtDNA damage in diabetes. Moreover, interactions of p66Shc with Pin1 are also increased, further strengthening the role of p66Shc in mitochondrial dysfunction. Consistent with our results, others have shown protection of hyperglycemia-induced mitochondrial oxidative stress and vascular dysfunction by regulation of Pin1 in human aortic endothelial cells, or knockout of *Pin1* in mouse (9, 46).

In conclusion, using *in vitro* and *in vivo* models of diabetic retinopathy, we have provided a mechanism of p66Shc activation in diabetes, and have demonstrated a significant role of p66Shc in the regulation of oxidative stress in the development

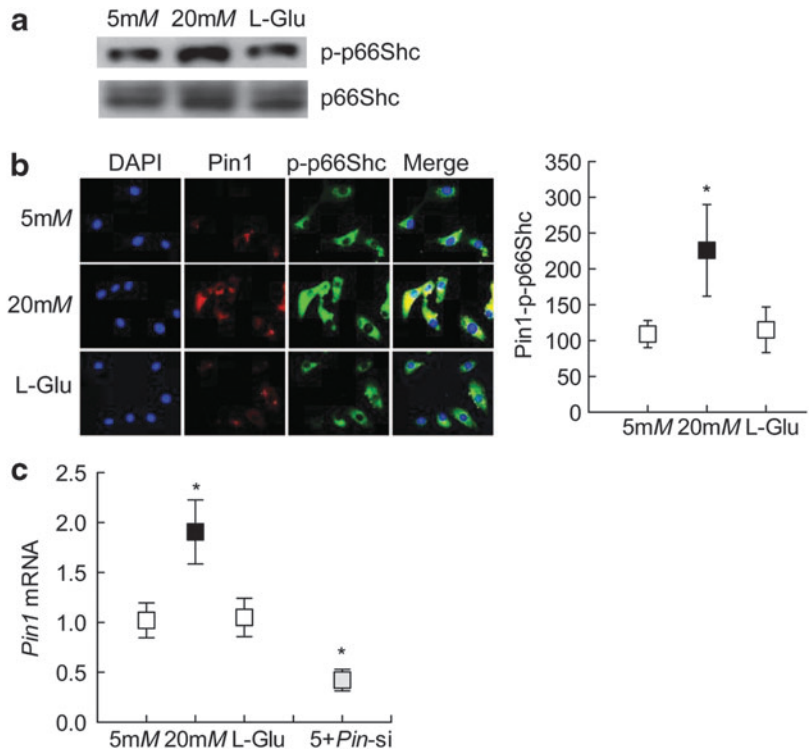

FIG. 6. Phosphorylation of *p66Shc*. (a) Phosphorylation of p66Shc (p-p66Shc) was determined by Western blot technique. Supplementary Figure S5 shows uncropped p-p66Shc Western blots from three different samples. **(b)** Interaction between Pin1 with p-p66Shc was determined by analyzing their cellular colocalization in immunofluorescence imaging using Texas Red (*red*) and DyLight 488 (*green*) conjugated secondary antibodies for Pin1 and p-p66Shc, respectively. **(c)** *Pin1* expression was quantified by qPCR using β-*Actin* as a housekeeping gene. Each measurement was made in duplicate in —three to five samples per group, and the values obtained from cells in 5 m*M* glucose are considered as 100 (or 1). $*p < 0.05$ compared with 5 m*M* glucose. Pin1, peptidyl-prolyl cis/trans isomerase 1.

of diabetic retinopathy. Owing to inhibition of Sirt1 in diabetes, acetylated H3K9 enhances p53 binding, inducing *p66Shc* expression. Increased cytosolic p66Shc increases in its binding with Grb2, which releases Sos1 from Sos1–Grb2 complex. This alters the GEF binding of Sos1 and activates Rac1. Active Rac1, *via* Nox2 activation, increases cytosolic ROS. In addition, p66Shc is phosphorylated, allowing it to localize in the mitochondria, and *via* interacting with Pin1, increases mitochondrial ROS (Fig. 9). Taken together, this study suggests that p66Shc is an essential regulator of both cytosolic and mitochondrial ROS, and provides a novel insight into the mechanism associated with increased mitochondrial dysfunction in the development of diabetic retinopathy.

Methods

Retinal endothelial cells

HRECs purchased from Cell Systems Corporation (Kirkland, WA) were grown in the growth medium containing modified Dulbecco's modified Eagle's medium (DMEM) F12 with normal glucose (5.5 m*M*), 12% heat-inactivated fetal bovine serum, 20 μg/mL endothelial cell growth supplement, and 1% each of insulin transferrin selenium, glutamax, and antibiotic/antimycotic (14, 40, 41). Cells from fifth to eighth passage were incubated in normal or high (20 m*M*) D-glucose (glucose) for 24–96 h, and parallel osmotic/metabolic controls included cells incubated in 20 m*M* L-glucose. The growth medium with reduced fetal bovine serum (1%) and endothelial growth factor (1 μg/mL), and 9% Nu-Serum was used as the normal glucose incubation medium. To prepare high-glucose incubation medium, 20 m*M* glucose was added to the normal glucose incubation medium. To investigate the effect of regulation of *p66Shc* on cellular ROS and mitochondrial damage, a batch of cells were transfected with specific siRNAs of *p66Shc* (20), *Sos1*, or *Pin1* using Lipofectamine RNAiMAX (Thermo Fisher Scientific, Rockford, IL), or with *Sirt1* plasmids (Sirt1 complementary DNA [cDNA], RC227720; OriGene, Rockville, MD), employing transfection reagent sc-29528 (Santa Cruz Biotechnology). All of the siRNAs (*p66Shc, a* custom-made siRNA; *Pin1,* Cat. No. EHU027711; *Sos1*, Cat EHU017831) were obtained from Sigma Chemicals (St. Louis, MO). After transfection, the cells were rinsed with DMEM and incubated in either 5 or 20 m*M* glucose for 96 h (14, 41). Parallel incubations with nontargeting scrambled RNA were used as controls. The efficiency of transfection was determined by quantifying their gene transcription using SYBR green-based quantitative real-time polymerase chain reaction (qPCR).

Rats

Wistar rats (male, body weight 200 g) were injected streptozotocin (intraperitoneal, 55 mg/kg body weight), and diabetic rats received 1–2 IU insulin four to five times a week to prevent ketosis and weight loss (31–33). At the end of 5–6 months of diabetes (blood glucose >250 mg/dL, 80–125 mL urine/24 h), the animals were euthanized by CO_2 inhalation, and the retina from one eye was crosslinked with 1% paraformaldehyde for immunohistochemical analysis and that from other eye was utilized for microvessel preparation for molecular parameters. Age-matched normal rats (blood glucose 80–100 mg/dL, 10–25 mL urine/24 h) served as controls. Treatment of animals conformed to the ARVO Statement for the Use of Animals in Ophthalmic and Vision Research, and Institutional Animal Care and Use Committee (Wayne State University, Detroit, MI). Microvessels were prepared using hypotonic shock method by incubating the retina in 5–6 mL deionized water for 60 min at 37°C in a shaking water bath. Vascular architecture

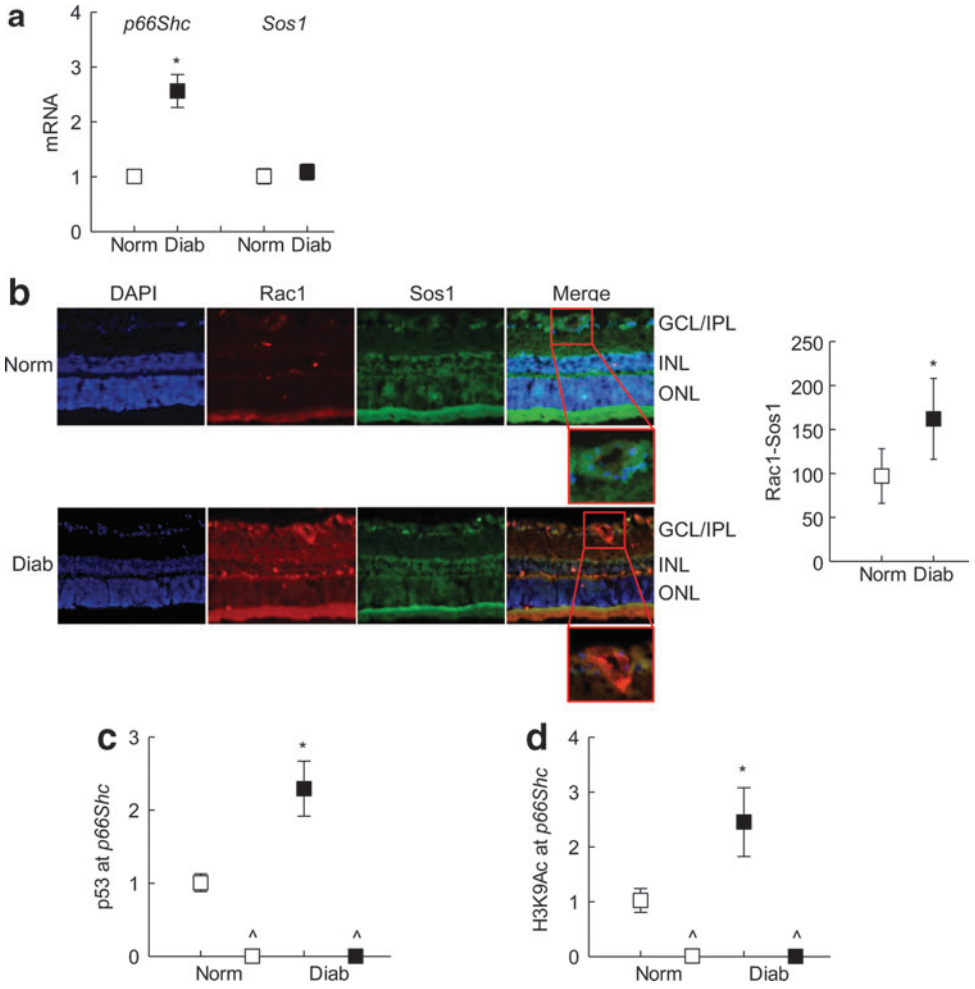

FIG. 7. Effect of diabetes on *p66Shc* and p53 binding at its promoter. Retina from streptozotocin-induced diabetic rats was used to prepare **(a)** microvessels by the hypotonic shock method. Transcripts of *p66Shc* and *Sos1* were quantified by qPCR using β-*Actin* as a housekeeping gene and **(b)** cryosections (8 μm) to analyze Rac1 interaction with Sos1 by immunofluorescence staining using Texas Red (*red*) and DyLight 488 (*green*) labeled secondary antibodies, respectively. Fluorescence intensity of the colocalized p66Shc-Rac1 was quantified; the *insets* show magnified vascular areas. **(c)** P53 binding and **(d)** H3K9Ac at *p66Shc* promoter were determined in retinal microvessels by ChIP assay. Values obtained from normal rat retinal microvessels are considered as 1 (or 100%), and are mean ± SD of five to six mice per group. $*p < 0.05$ compared with normal. GCL/IPL, ganglion cell layer/inner plexiform layer; INL, inner nuclear layer; Norm and Diab, normal and diabetic rats, respectively; ONL, outer nuclear layer.

was gently cleared for nonvascular debris under the microscope and used for analyses (39).

Gene transcripts

Levels of mRNA were quantified by qPCR using target-specific primers (Table 1) and following standard laboratory amplification condition for cDNA or immunoprecipitated DNA. Reaction specificity was validated by a single peak in the melting curve. Values of the products were normalized to the cycle threshold (Ct) value from the input sample, and those in cDNA to the Ct values from β-*Actin* in the same sample (41).

Western blot

Protein (40 μg) was separated on a 4–20% gradient acrylamide gel (BioRad, Hercules, CA) and transferred onto nitrocellulose membranes. Protein expression was detected using the following antibodies: rabbit anti-p66Shc (1:1000), anti-Sos1 (1:1000), anti-Grb2 (1:1000), anti-Pin1 (1:1000), and mouse antiserine 36 phosphorylated p66Shc (1:500; Cat. Nos. ab33770, ab54518, ab140621, ab32037, and ab76309, respectively; Abcam, Cambridge, MA), and mouse anti-β-Actin (1:2000; Cat. No. A5441; Sigma Chemicals) was used as a loading protein. Relative expression of the target proteins was normalized against β-Actin, and the band intensities were quantified using Image J software (52).

Protein–protein interaction

Interactions of Sos1 with Rac1 and of Sos1 with Grb2 were quantified by immunoprecipitating Rac1 or Grb2 using 3 μg of their respective antibodies (Rac1 antibody Cat. No. PA1-091; Thermo Fisher Scientific and Sos1 and Grb2 antibodies, the same as used for the Western blotting). This was followed by incubation with Protein A/G Plus agarose beads. After washing the beads, the proteins were separated on a sodium dodecyl sulfate–polyacrylamide gel electrophoresis, and were immunoblotted for Sos1, following the standard procedures routinely used in the laboratory (41).

Retinal cryosection

Enucleated eye balls were washed in phosphate buffered saline (PBS) and fixed in 4% paraformaldehyde for 4 h. After three washes with PBS, they were incubated overnight at 4°C in 5% sucrose, and this was followed by incubations in 10% and 15% sucrose each for 1 h. The tissue was then incubated overnight at 4°C in a solution containing equal volumes of 20% sucrose and optimal cutting temperature (OCT) medium. Finally, it was casted onto OCT medium in a mold and

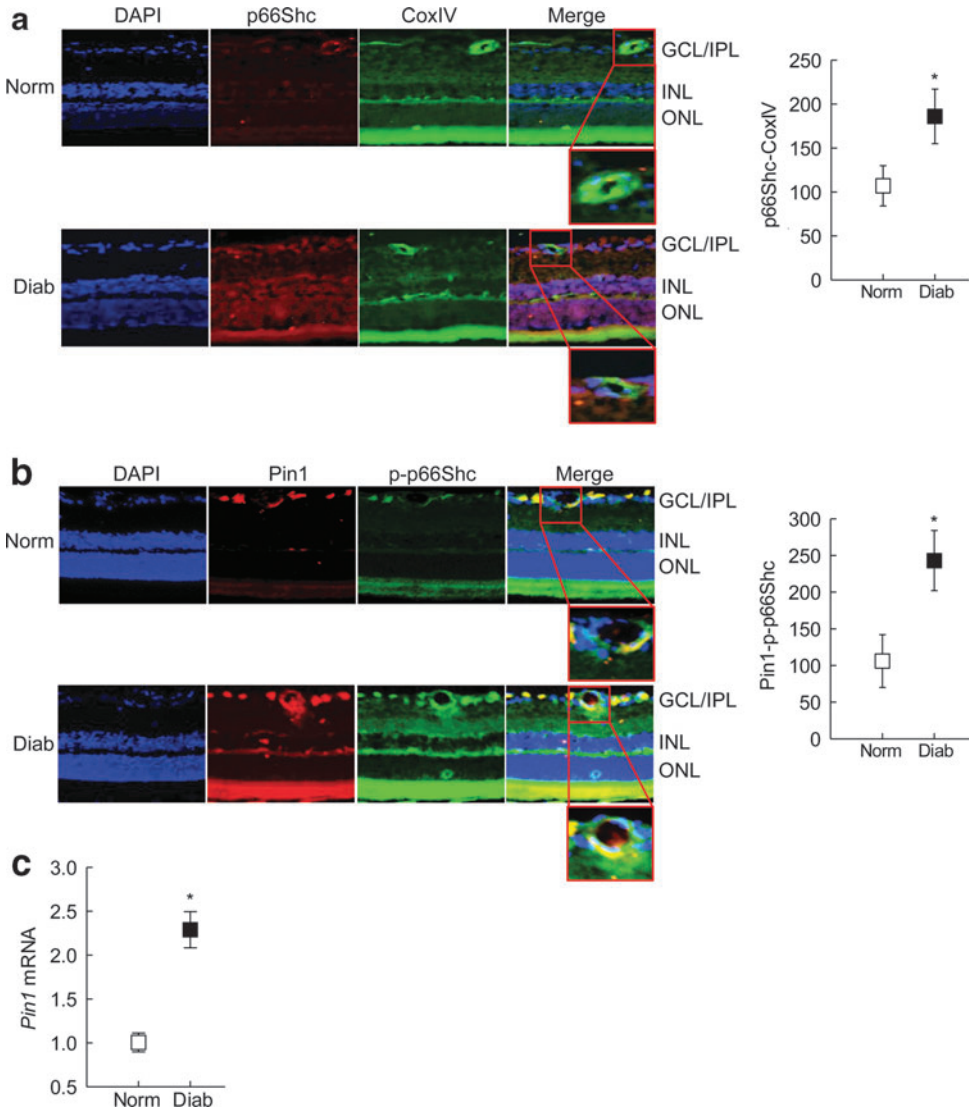

FIG. 8. Mitochondrial localization of *p66Shc* in diabetes. (a) Mitochondrial localization of p66Shc was quantified in the rat retinal cryosections by immunofluorescence staining using Texas Red and DyLight 488 labeled secondary antibodies for p66Shc and CoxIV (mitochondrial marker), respectively. **(b)** Pin1p-p66Shc colocalization was quantified by immunofluorescence staining using Texas Red and DyLight 488 labeled secondary antibodies, respectively, the *insets* show magnified vascular areas. **(c)** Pin1 expression in retinal microvessels (hypotonic shock) was quantified by qPCR using β-*Actin* as a housekeeping gene. Values are represented as mean ± SD from five to six rats per group. $*p < 0.05$ compared with normal.

kept at −20°C. Using cryotome, 8 μM thick retinal sections were prepared for immunofluorescence analysis (39).

Immunofluorescence imaging

Cellular colocalization of Sos1-Rac1 and Pin1-phosphorylated p66Shc was examined in crosslinked HRECs or retinal cryosections by immunofluorescence technique using target-specific primary antibodies (the same antibodies as used for Western blotting) and DyLight 488 (green) or Texas-red (red)-conjugated secondary antibodies. The primary antibodies were diluted 1:200, and the secondary antibodies were diluted 1:500. Mitochondrial localization of p66Shc was examined using CoxIV (1:200; Cat. No. sc58348; Santa Cruz Biotechnology) as a mitochondrial marker. Immunolabeled cells were mounted using DAPI-containing (blue) VECTASHIELD mounting medium (Vector Laboratories, Burlingame, CA), and the slides were imaged under a Zeiss ApoTome fluorescence microscope using 40× magnification (39, 41). Fluorescence intensity was quantified using Axiovision Rel 4.8 software.

Isolation of mitochondria

Mitochondria were prepared using mitochondria isolation kit from ThermoFisher (Pierce, Rockford, IL) (33). In brief, after digesting the homogenized samples with the kit reagents, samples were centrifuged at 700 × *g* for 10 min, followed by centrifugation at 3000 × *g* for 15 min. The pellet thus obtained was washed, suspended in PBS, and used for the quantification of mitochondrial ROS.

Active Rac1 assay

Active Rac1 was quantified using the G-LISA colorimetric assay kit (Cytoskeleton, Denver, CO), as described previously (32, 34).

ROS quantification

ROS were quantified fluorometrically using dichlorodihydrofluorescein diacetate (DCFH-DA). In brief, 5 μg protein (homogenate or mitochondria) was incubated with 4 μM DCFH-DA

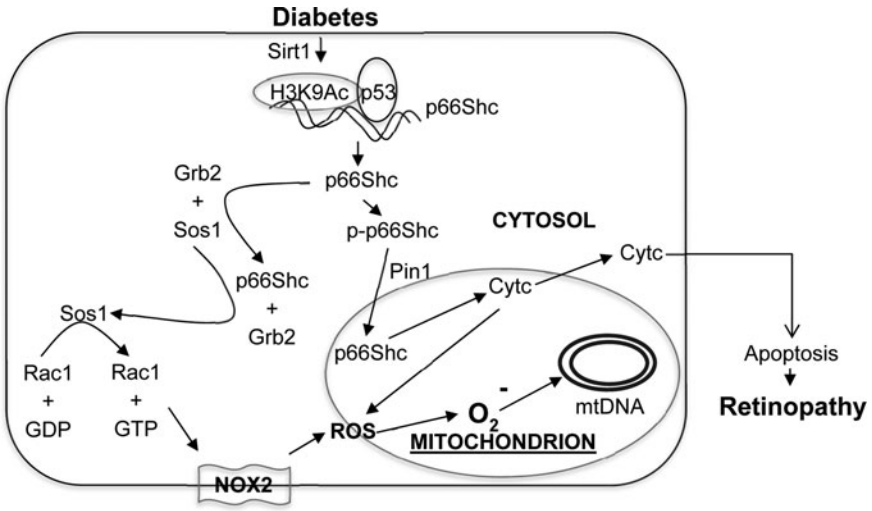

FIG. 9. A schematic of the signaling events. Our model shows that in diabetes, decreased expression of Sirt1 increases H3K9 acetylation at *p66Shc* promoter and p53 transcription factor binding, which subsequently increases *p66Shc* expression. Cytosolic accumulation of p66Shc leads to increase in its binding with Grb2 and releasing Sos1 from Sos1–Grb2 complex. Sos1, thus, by replacing GDP with GTP, activates Rac1 and consequently induces Nox2-mediated cytosolic ROS production. In addition, increased p66Shc phosphorylation (p-p66Shc) facilitates its Pin1-mediated isomerization and mitochondrial localization. In mitochondria, it oxidizes Cyt c, generates ROS, and damages mitochondrial DNA and membranes. Cyt c release in the cytoplasm is increased, activating the apoptotic machinery, and ultimately, the development of retinopathy. Cyt c, cytochrome c; GDP, guanosine diphosphate; GTP, guanosine triphosphate; Nox, NADPH oxidase.

for 10 min, and fluorescence was measured at 485 nm excitation and 535 nm as emission wavelengths (32, 33).

Mitochondrial ROS were also quantified in the live HRECs using MitoSOX™ red mitochondrial superoxide indicator and mitotracker green as the mitochondrial marker (44, 54). In brief, the cells were washed with PBS, and incubated with 5 μM MitoSOX red and 200 nM mitotracker green (Thermo Fisher Scientific) for 10 min at 37°C. The fluorescence was examined under a Zeiss ApoTome using 40× objective. HRECs incubated in 5 μM MitoSOX red maintained their phenotype, and the results using 2 μM MitoSOX red were not different from those using 5 μM MitoSOX red.

Table 1. Primer Sequence

Gene	*Sequence*
Human	
p66Shc	5′-TCTCTGTCATCGCTGGAGGA-3′
	5′-ATGAAGCTGATGGGGAAGGC-3′
Sos1	5′-CCCCGGGGGCACCAT-3′
	5′-GGATGAACTTGCCCCTGGAC-3′
Grb2	5′-AAGCTACTGCAGACGACGAG-3′
	5′-CTTGGCTCTGGGGATTTTGC-3′
Pin1	5′-CAGAGCGCGTCTAGCCA-3′
	5′-TGGTTGAAGTAGTACACTCGGC-3′
p53 at *p66Shc* promoter	5′-GATTTCAGCAACGCGAGCAG-3′
	5′-AAAGGTGGCCGGAGGTTGTA-3′
β-*Actin*	5′-AGCCTCGCCTTTGCCGATCCG-3′
	5′-TCTCTTGCTCTGGGCCTCGTCG-3′
Rat	
p66Shc	5′-GACTAGGCTAAGGGTCTGGG-3′
	5′-CCTCCTCCAGCGATGACAGA-3′
Sos1	5′-GTCTGCAGCGTGTTCGATTC-3′
	5′-GGCAGACTCTGGTCGTCTTC-3′
Pin1	5′-AGAAGCGTATGAGTCGCAGC-3′
	5′-CTCCGAGATTGGCTGTGCTT-3′
p53 at *p66Shc* promoter	5′-CCCCTTCCTTACACAAGCCA-3′
	5′-GGGAGAACGTAGCAAAAGCG-3′
β-*Actin*	5′-CCTCTATGCCAACACAGTGC-3′
	5′-CATCGTACTCCTGCTTGCTG-3′

Grb2, growth factor receptor-bound protein 2; Pin1, peptidyl-prolyl cis/trans isomerase 1; Sos1, Son of Sevenless 1.

Oxidatively modified DNA

OHdG levels were measured using an ELISA kit from OXIS Research (8-OHdG-EIA, Portland, OR), as described by us previously (31). DNA isolated by the phenol–chloroform method was suspended in the elution buffer. 8-OHdG standard (2–200 ng/mL) or 2.0 μg DNA was incubated at 37°C for 1 h with monoclonal antibody against 8-OHdG in a microtiter plate precoated with 8-OHdG. The final color was developed by the addition of 3, 3′, 5, 5′-tetramethylbenzidine, and absorbance was measured at 450 nm.

Chromatin immunoprecipitation

Chromatin immunoprecipitation was performed using a kit from Millipore Corp. (Temecula, CA). In brief, immunoprecipitated protein–DNA complex (120 μg) was incubated with 3 μg antibody against H3K9Ac or p53 (Cat. Nos. ab4441, ab1101; Abcam). DNA fragments were recovered by phenol–chloroform–isoamyl alcohol; ethanol precipitated and was analyzed by qPCR. Normal rabbit IgG was used as negative antibody control and DNA from the input (20 μg protein–DNA complex) was used as an internal control (40, 41).

Mitochondrial damage

Genome-specific quantitative extended length PCR was performed to assess mtDNA damage using the methods reported previously (32). In brief, long (8.8 kb) and short (223 bp)

mtDNA regions were amplified using semiquantitative PCR, and the amplified products were resolved on agarose gel. Relative amplification was quantified by normalizing the intensity of the short product to the long product (223 bp/8.8 kb).

Apoptosis

Cell apoptosis was determined by quantifying the presence of oligonucleosomes in the cytosolic fraction of the cells using monoclonal antibodies directed against DNA and histones, followed by incubation in a mixture of peroxidase-conjugated anti-DNA and biotin-labeled antihistone in a streptavidin-coated plate (Cell Death Detection ELISAPLUS kit; Roche Diagnostics, Indianapolis, IN). The plate was washed thoroughly, incubated with 2, 20-azino-di-[3-ethylbenzthiazoline sulfonate] diammonium salt, and the absorbance was measured at 405 nm (32, 39).

Statistical analysis

Results were analyzed using Sigma Stat software (San Jose, CA), and the data are presented as mean ± standard deviations. Statistical test between two groups was carried out by *t*-test or Mann–Whitney rank-sum test. For multiple comparisons for the data with normal distribution, one-way analysis of variance followed by Student–Newman–Keul's test was performed; $p < 0.05$ was considered as statistically significant.

Acknowledgments

The authors acknowledge the grants support from the National Institutes of Health (R01-EY014370, R01-EY017313, and R01-EY022230) and the Thomas Foundation to R.A.K., and from Research to Prevent Blindness to the Ophthalmology Department.

Author Disclosure Statement

All authors do not have any conflict of interest.

References

1. Ahmed SBM and Prigent SA. Insights into the Shc family of adaptor proteins. *J Mol Signal* 12: 2, 2017.
2. Arany I, Faisal A, Nagamine Y, and Safirstein RL. p66shc inhibits pro-survival epidermal growth factor receptor/ERK signaling during severe oxidative stress in mouse renal proximal tubule cells. *J Biol Chem* 283: 6110–6117, 2008.
3. Beltrami E, Valtorta S, Moresco R, Marcu R, Belloli S, Fassina A, Fazio F, Pelicci P, and Giorgio M. The p53-p66Shc apoptotic pathway is dispensable for tumor suppression whereas the p66Shc-generated oxidative stress initiates tumorigenesis. *Curr Pharm Des* 19: 2708–2714, 2013.
4. Bhat HF, Baba RA, Adams ME, and Khanday FA. Role of SNTA1 in Rac1 activation, modulation of ROS generation, and migratory potential of human breast cancer cells. *Br J Cancer* 110: 706–714, 2014.
5. Bhat SS, Anand D, and Khanday FA. p66Shc as a switch in bringing about contrasting responses in cell growth: implications on cell proliferation and apoptosis. *Mol Cancer* 14: 76, 2015.
6. Bhaumik SR, Smith E, and Shilatifard A. Covalent modifications of histones during development and disease pathogenesis. *Nat Struct Mol Biol* 14: 1008–1016, 2007.
7. Carlomosti F, D'Agostino M, Beji S, Torcinaro A, Rizzi R, Zaccagnini G, Maimone B, Di Stefano V, De Santa F, Cordisco S, Antonini A, Ciarapica R, Dellambra E, Martelli F, Avitabile D, Capogrossi MC, and Magenta A. Oxidative stress-induced miR-200c disrupts the regulatory loop among SIRT1, FOXO1, and eNOS. *Antioxid Redox Signal* 27: 328–344, 2017.
8. Chen H, Wan Y, Zhou S, Lu Y, Zhang Z, Zhang R, Chen F, Hao D, Zhao X, Guo Z, Liu D, and Liang C. Endothelium-specific SIRT1 overexpression inhibits hyperglycemia-induced upregulation of vascular cell senescence. *Sci China Life Sci* 55: 467–473, 2012.
9. Costantino S, Paneni F, Lüscher TF, and Cosentino F. Pin1 inhibitor Juglone prevents diabetic vascular dysfunction. *Int J Cardiol* 203: 702–707, 2016.
10. Costantino S, Paneni F, Virdis A, Hussain S, Mohammed SA, Capretti G, Akhmedov A, Dalgaard K, Chiandotto S, Pospisilik JA, Jenuwein T, Giorgio M, Volpe M, Taddei S, Lüscher TF, and Cosentino F. Interplay among H3K9-editing enzymes SUV39H1, JMJD2C and SRC-1 drives p66Shc transcription and vascular oxidative stress in obesity. *Eur Heart J* 40: 383–391, 2019.
11. Daiber A. Redox signaling (cross-talk) from and to mitochondria involves mitochondrial pores and reactive oxygen species. *Biochim Biophys Acta* 1797: 897–906, 2010.
12. Daiber A, Di Lisa F, Oelze M, Kröller-Schön S, Steven S, Schulz E, and Münzel T. Crosstalk of mitochondria with NADPH oxidase via reactive oxygen and nitrogen species signalling and its role for vascular function. *Br J Pharmacol* 174: 1670–1689, 2017.
13. Dikalov S. Cross talk between mitochondria and NADPH oxidases. *Free Radic Biol Med* 51: 1289–1301, 2011.
14. Duraisamy AJ, Mishra M, and Kowluru RA. Crosstalk between histone and DNA methylation in regulation of retinal matrix metalloproteinase-9 in diabetes. *Invest Ophthalmol Vis Sci* 58: 6440–6448, 2017.
15. Feng D, Yao J, Wang G, Li Z, Zu G, Li Y, Luo F, Ning S, Qasim W, Chen Z, and Tian X. Inhibition of p66Shc-mediated mitochondrial apoptosis via targeting prolyl-isomerase Pin1 attenuates intestinal ischemia/reperfusion injury in rats. *Clin Sci (Lond)* 131: 759–773, 2017.
16. Frank RN. Diabetic retinopathy. *N Engl J Med* 350: 48–58, 2004.
17. Galimov ER. The role of p66shc in oxidative stress and apoptosis. *Acta Nat* 2: 44–51, 2010.
18. Giacco F and Brownlee M. Oxidative stress and diabetic complications. *Circ Res* 107: 1058–1070, 2010.
19. Giorgio M, Migliaccio E, Orsini F, Paolucci D, Moroni M, Contursi C, Pelliccia G, Luzi L, Minucci S, Marcaccio M, Pinton P, Rizzuto R, Bernardi P, Paolucci F, and Pelicci PG. Electron transfer between cytochrome c and p66Shc generates reactive oxygen species that trigger mitochondrial apoptosis. *Cell* 122: 221–233, 2005.
20. Haines E, Saucier C, and Claing A. The adaptor proteins p66Shc and Grb2 regulate the activation of the GTPases ARF1 and ARF6 in invasive breast cancer cells. *J Biol Chem* 289: 5687–5703, 2014.
21. Ingersoll MA, Chou YW, Lin JS, Yuan TC, Miller DR, Xie Y, Tu Y, Oberley-Deegan RE, Batra SK, and Lin MF. p66Shc regulates migration of castration-resistant prostate cancer cells. *Cell Signal* 46: 1–14, 2018.
22. Kadiyala CS, Zheng L, Du Y, Yohannes E, Kao HY, Miyagi M, and Kern TS. Acetylation of retinal histones in diabetes increases inflammatory proteins: effects of

minocycline and manipulation of histone acetyltransferase (HAT) and histone deacetylase (HDAC). *J Biol Chem* 287: 25869–25880, 2012.
23. Khanday FA, Santhanam L, Kasuno K, Yamamori T, Naqvi A, Dericco J, Bugayenko A, Mattagajasingh I, Disanza A, Scita G, and Irani K. Sos-mediated activation of rac1 by p66shc. *J Cell Biol* 172: 817–822, 2006.
24. Khanday FA, Yamamori T, Mattagajasingh I, Zhang Z, Bugayenko A, Naqvi A, Santhanam L, Nabi N, Kasuno K, Day BW, and Irani K. Rac1 leads to phosphorylation-dependent increase in stability of the p66shc adaptor protein: role in Rac1-induced oxidative stress. *Mol Biol Cell* 17: 122–129, 2006.
25. Kim CS, Jung SB, Naqvi A, Hoffman TA, DeRicco J, Yamamori T, Cole MP, Jeon BH, and Irani K. p53 impairs endothelium-dependent vasomotor function through transcriptional upregulation of p66shc. *Circ Res* 103: 1441–1450, 2008.
26. Kim YM, Kim SJ, Tatsunami R, Yamamura H, Fukai T, and Ushio-Fukai M. ROS-induced ROS release orchestrated by Nox4, Nox2, and mitochondria in VEGF signaling and angiogenesis. *Am J Physiol Cell Physiol* 312: C749–C764, 2017.
27. Kirmani D, Bhat HF, Bashir M, Zargar MA, and Khanday FA. P66Shc-rac1 pathway-mediated ROS production and cell migration is downregulated by ascorbic acid. *J Recept Signal Transduct Res* 33: 107–113, 2013.
28. Kowluru RA and Abbas SN. Diabetes-induced mitochondrial dysfunction in the retina. *Invest Ophthalmol Vis Sci* 44: 5327–5334, 2003.
29. Kowluru RA, Atasi L, and Ho YS. Role of mitochondrial superoxide dismutase in the development of diabetic retinopathy. *Invest Ophthalmol Vis Sci* 47: 1594–1599, 2006.
30. Kowluru RA, Jirousek MR, Stramm L, Farid N, Engerman RL, and Kern TS. Abnormalities of retinal metabolism in diabetes or experimental galactosemia: V. Relationship between protein kinase C and ATPases. *Diabetes* 47: 464–469, 1998.
31. Kowluru RA and Kanwar M. Effect of curcumin on retinal oxidative stress and inflammation in diabetes. *Nutr Metab (Lond)* 4: 1–8, 2007.
32. Kowluru RA, Kowluru A, Veluthakal R, Mohammad G, Syed I, Santos JM, and Mishra M. TIAM1-RAC1 signalling axis-mediated activation of NADPH oxidase-2 initiates mitochondrial damage in the development of diabetic retinopathy. *Diabetologia* 57: 1047–1056, 2014.
33. Kowluru RA, Mishra M, Kowluru A, and Kumar B. Hyperlipidemia and the development of diabetic retinopathy: comparison between type 1 and type 2 animal models. *Metabolism* 65: 1570–1581, 2016.
34. Kumar B, Kowluru A, and Kowluru RA. Lipotoxicity augments glucotoxicity-induced mitochondrial damage in the development of diabetic retinopathy. *Invest Ophthalmol Vis Sci* 56: 2985–2992, 2015.
35. Kumar S, Kim YR, Vikram A, Naqvi A, Li Q, Kassan M, Kumar V, Bachschmid MM, Jacobs JS, Kumar A, and Irani K. Sirtuin1-regulated lysine acetylation of p66Shc governs diabetes-induced vascular oxidative stress and endothelial dysfunction. *Proc Natl Acad Sci U S A* 114: 1714–1719, 2017.
36. Li J, Wang JJ, Yu Q, Chen K, Mahadev K, and Zhang SX. Inhibition of reactive oxygen species by lovastatin downregulates VEGF expression and ameliorates blood-retinal barrier breakdown in db/db mice: role of NADPH oxidase 4. *Diabetes* 59: 1528–1538, 2010.
37. Liao B, Zhang Y, Sun H, Ma B, and Qian J. Ryanodine receptor 2 plays a critical role in spinal cord injury via induction of oxidative stress. *Cell Physiol Biochem* 38: 1129–1137, 2016.
38. Menini S, Amadio L, Oddi G, Ricci C, Pesce C, Pugliese F, Giorgio M, Migliaccio E, Pelicci P, Iacobini C, and Pugliese G. Deletion of p66Shc longevity gene protects against experimental diabetic glomerulopathy by preventing diabetes-induced oxidative stress. *Diabetes* 55: 1642–1650, 2006.
39. Mishra M, Duraisamy AJ, and Kowluru RA. Sirt1: a guardian of the development of diabetic retinopathy. *Diabetes* 67: 745–754, 2018.
40. Mishra M and Kowluru RA. The role of DNA methylation in the metabolic memory phenomenon associated with the continued progression of diabetic retinopathy. *Invest Ophthalmol Vis Sci* 57: 5748–5757, 2016.
41. Mishra M and Kowluru RA. Role of PARP-1 as a novel transcriptional regulator of MMP-9 in diabetic retinopathy. *Biochim Biophys Acta* 1863: 1761–1769, 2017.
42. Miyazawa M and Tsuji Y. Evidence for a novel antioxidant function and isoform-specific regulation of the human p66Shc gene. *Mol Biol Cell* 25: 2116–2127, 2014.
43. Mizutani M, Kern TS, and Lorenzi M. Accelerated death of retinal microvascular cells in human and experimental diabetic retinopathy. *J Clin Invest* 97: 2883–2890, 1996.
44. Mukherjee P, Woods TA, Moore RA, and Peterson KE. Activation of the innate signaling molecule MAVS by bunyavirus infection upregulates the adaptor protein SARM1, leading to neuronal death. *Immunity* 38: 705–716, 2013.
45. Pagnin E, Fadini G, de Toni R, Tiengo A, Calò L, and Avogaro A. Diabetes induces p66shc gene expression in human peripheral blood mononuclear cells: relationship to oxidative stress. *J Clin Endocrinol Metab* 90: 1130–1136, 2005.
46. Paneni F, Costantino S, Castello L, Battista R, Capretti G, Chiandotto S, D'Amario D, Scavone G, Villano A, Rustighi A, Crea F, Pitocco D, Lanza G, Volpe M, Del Sal G, Lüscher TF, and Cosentino F. Targeting prolyl-isomerase Pin1 prevents mitochondrial oxidative stress and vascular dysfunction: insights in patients with diabetes. *Eur Heart J* 36: 817–828, 2015.
47. Pellegrini M, Pacini S, and Baldari CT. p66SHC: the apoptotic side of Shc proteins. *Apoptosis* 10: 13–18, 2005.
48. Pinton P, Rimessi A, Marchi S, Orsini F, Migliaccio E, Giorgio M, Contursi C, Minucci S, Mantovani F, Wieckowski MR, Del Sal G, Pelicci PG, and Rizzuto R. Protein kinase C beta and prolyl isomerase 1 regulate mitochondrial effects of the life-span determinant p66Shc. *Science* 315: 659–663, 2007.
49. Saha A, Wittmeyer J, and Cairns BR. Chromatin remodelling: the industrial revolution of DNA around histones. *Nat Rev Mol Cell Biol* 7: 437–447, 2006.
50. Sarfstein R, Gorzalczany Y, Mizrahi A, Berdichevsky Y, Molshanski-Mor S, Weinbaum C, Hirshberg M, Dagher MC, and Pick E. Dual role of Rac in the assembly of NADPH oxidase, tethering to the membrane and activation of p67phox: a study based on mutagenesis of p67phox-Rac1 chimeras. *J Biol Chem* 279: 16007–16016, 2004.
51. Saunders LR and Verdin E. Sirtuins: critical regulators at the crossroads between cancer and aging. *Oncogene* 26: 5489–5504, 2007.
52. Schneider CA, Rasband WS, and Eliceiri KW. NIH Image to ImageJ: 25 years of image analysis. *Nat Methods* 9: 671–675, 2012.
53. Schulz E, Wenzel P, Münzel T, and Daiber A. Mitochondrial redox signaling: interaction of mitochondrial reactive

oxygen species with other sources of oxidative stress. *Antioxid Redox Signal* 20: 308–324, 2014.
54. Sena LA, Li S, Jairaman A, Prakriya M, Ezponda T, Hildeman DA, Wang CR, Schumacker PT, Licht JD, Perlman H, Bryce PJ, and Chandel NS. Mitochondria are required for antigen-specific T cell activation through reactive oxygen species signaling. *Immunity* 38: 225–236, 2013.
55. Tait SW and Green DR. Mitochondria and cell death: outer membrane permeabilization and beyond. *Nat Rev Mol Cell Biol* 11: 621–632, 2010.
56. Toledo F and Wahl GM. Regulating the p53 pathway: in vitro hypotheses, in vivo veritas. *Nat Rev Cancer* 6: 909–923, 2006.
57. Trinei M, Giorgio M, Cicalese A, Barozzi S, Ventura A, Migliaccio E, Milia E, Padura IM, Raker VA, Maccarana M, Petronilli V, Minucci S, Bernardi P, Lanfrancone L, and Pelicci PG. A p53-p66Shc signalling pathway controls intracellular redox status, levels of oxidation-damaged DNA and oxidative stress-induced apoptosis. *Oncogene* 21: 3872–3878, 2002.
58. Whetstine JR, Ceron J, Ladd B, Dufourcq P, Reinke V, and Shi Y. Regulation of tissue-specific and extracellular matrix-related genes by a class I histone deacetylase. *Mol Cell* 18: 483–490, 2005.
59. Wils J, Favre J, and Bellien J. Modulating putative endothelial progenitor cells for the treatment of endothelial dysfunction and cardiovascular complications in diabetes. *Pharmacol Ther* 170: 98–115, 2017.
60. Xu W, Zhuang Z, Yang J, Yang L, Xu Y, and Zhang W. Profile of P66SHC expression and histone modifications in replicative cell senescence and oxidative-stress induced premature senescence. *Wei Sheng Yan Jiu* 42: 777–782, 2013.
61. Xu X, Zhu X, Ma M, Han Y, Hu C, Yuan S, Yang Y, Xiao L, Liu F, Kanwar YS, and Sun L. p66Shc: a novel biomarker of tubular oxidative injury in patients with diabetic nephropathy. *Sci Rep* 6: 29302, 2016.
62. Zhou S, Chen HZ, Wan YZ, Zhang QJ, Wei YS, Huang S, Liu JJ, Lu YB, Zhang ZQ, Yang RF, Zhang R, Cai H, Liu DP, and Liang CC. Repression of P66Shc expression by SIRT1 contributes to the prevention of hyperglycemia-induced endothelial dysfunction. *Circ Res* 109: 639–648, 2011.
63. Zorov DB, Filburn CR, Klotz LO, Zweier JL, and Sollott SJ. Reactive oxygen species (ROS)-induced ROS release: a new phenomenon accompanying induction of the mitochondrial permeability transition in cardiac myocytes. *J Exp Med* 192: 1001–1014, 2000.
64. Zorov DB, Juhaszova M, and Sollott SJ. Mitochondrial reactive oxygen species (ROS) and ROS-induced ROS release. *Physiol Rev* 94: 909–950, 2014.

Address correspondence to:
Dr. Renu A. Kowluru
Kresge Eye Institute
Wayne State University
4717 St. Antoine, Detroit, MI 48201

E-mail: rkowluru@med.wayne.edu

Date of first submission to ARS Central, March 14, 2018; date of final revised submission, July 23, 2018; date of acceptance, August 10, 2018.

Abbreviations Used

cDNA = complementary DNA
CH2 = collagen homology-2
Ct = cycle threshold
Cyt c = cytochrome c
DCFH-DA = dichlorodihydrofluorescein diacetate
DMEM = Dulbecco's modified Eagle's medium
ELISA = enzyme-linked immunosorbent assay
GEF = guanine exchange factor
Grb2 = growth factor receptor-bound protein 2
H3K9Ac = histone 3 lysine 9 acetylation
HRECs = human retinal endothelial cells
mRNA = messenger RNA
mtDNA = mitochondrial DNA
Nox = NADPH oxidase
OCT = optimal cutting temperature
PBS = phosphate buffered saline
Pin1 = peptidyl-prolyl cis/trans isomerase 1
PKCβ = protein kinase C, β-isoform
qPCR = quantitative real-time polymerase chain reaction
Rac1 = Ras-related C3 botulinum toxin substrate 1
ROS = reactive oxygen species
siRNA = small interfering RNA
Sirt1 = sirtuin 1
Sos1 = Son of Sevenless 1